Mutual independence of water and n-nonane nucleation at low temperatures

Author(s):
Feusi, Stefan; Krohn, Jan; Li, Chenxi; Signorell, Ruth

Publication date:
2023-02-21

Permanent link:
https://doi.org/10.3929/ethz-b-000597374

Originally published in:
The Journal of Chemical Physics 158(7), https://doi.org/10.1063/5.0138628

Funding acknowledgement:
200306 - How weak intermolecular interactions govern the formation and properties of clusters and aerosol droplets (SNF)

The Journal of Chemical Physics ARTICLE scitation.org/journal/jcp

Mutual independence of water and *n*-nonane nucleation at low temperatures

Cite as: J. Chem. Phys. 158, 074301 (2023); doi: 10.1063/5.0138628
Submitted: 13 December 2022 • Accepted: 24 January 2023 •
Published Online: 15 February 2023

Stefan Feusi,[1] Jan Krohn,[1] Chenxi Li,[2] and Ruth Signorell[1,a)]

AFFILIATIONS

[1]Department of Chemistry and Applied Biosciences, Laboratory of Physical Chemistry, ETH Zürich, CH-8093 Zürich, Switzerland
[2]School of Environmental Science and Engineering, Shanghai Jiao Tong University, Shanghai 200240, China

Note: This paper is part of the JCP Special Topic on Nucleation: Current Understanding Approaching 150 Years After Gibbs.
[a)]**Author to whom correspondence should be addressed:** rsignorell@ethz.ch

ABSTRACT

The interaction of water with different substances in the earth's atmosphere lies at the heart of many processes that influence our climate. However, it is still unclear how different species interact with water on the molecular level and in which ways this interaction contributes to the water vapor phase transition. Here, we report the first measurements of water–nonane binary nucleation in the 50–110 K temperature range, along with unary nucleation data of both. The time-dependent cluster size distribution in a uniform post-nozzle flow was measured by time-of-flight mass spectrometry coupled with single-photon ionization. From these data, we extract experimental rates and rate constants for both nucleation and cluster growth. The observed mass spectra of water/nonane clusters are not or only slightly affected by the introduction of the other vapor, and the formation of mixed clusters was not observed during nucleation of the mixed vapor. Additionally, the nucleation rate of either substance is not much affected by the presence (or absence) of the other species, i.e., the nucleation of water and nonane proceeds independently, indicating that hetero-molecular clusters do not play a role during nucleation. Only at the lowest temperature of our experiment (i.e., 51 K) do the measurements suggest that interspecies interaction slows water cluster growth. The findings here are in contrast to our earlier work in which we showed that vapor components in other mixtures, e.g., CO_2 and toluene/H_2O, can interact to promote nucleation and cluster growth in a similar temperature range.

I. INTRODUCTION

The phase transition of water vapor plays a critical role in the earth's atmosphere, e.g., through cloud formation, which has profound impacts on the earth's radiative forcing and hydrological cycle.[1–4] During the past few decades, the unary nucleation of water vapor has been extensively studied for a wide range of temperatures.[5–7] These measurements suggest that the nucleation process of pure water vapor could be reasonably explained by the (modified) classical nucleation theory,[8,9] or modeled by the accurate determination of the dimerization rate constant.[10] However, in realistic systems (e.g., planetary atmospheres), water vapor coexists with other (trace) gaseous species. Water vapor nucleation can be strongly enhanced by these species, e.g., by sulfuric acid at near room temperature and by CO_2 at lower temperatures.[11,12] The degree of the enhancement depends on the ambient temperature, the concentration, and the molecular structure of the other species.

On a macroscopic level, water is immiscible with non-polar substances. It is of interest to examine if the immiscibility correlates with a lower strength of the non-polar substance's ability to enhance water nucleation (or vice versa, water's ability to enhance nucleation of the non-polar substance), which starts on a microscopic scale that involves small molecular clusters. *n*-Nonane is a non-polar organic species (in the following, *n*-nonane is simply referred to as nonane), and its liquid mixture with water has a pronounced miscibility gap.[13] Hence, the water–nonane vapor mixture can serve as a model system in which the intermolecular interactions between molecules of the same species are relatively strong but interspecies interactions are comparatively weak.

The nucleation of the water–nonane vapor mixture was systematically investigated by Wagner and Strey.[13] They observed a "two-pathway" behavior at 230 K, i.e., both substances nucleate along their unary nucleation pathway despite being in a vapor mixture. This observation is distinct from water–alcohol binary nucleation

in which mutual nucleation enhancement was observed,[14,15] but it is closer to nucleation of nonane mixtures with short chain alcohols in which the co-nucleation seems rather reluctant.[16] Additionally, at low gas phase activities of nonane, they observed a two-step behavior in which water clusters nucleate first and then serve as heterogeneous nuclei for the condensation of nonane; once nonane condenses on the particle, continued condensation of water is inhibited. Pathak *et al.*[17] studied binary water–nonane nucleation in a Laval expansion. They found a decrease of the water cluster concentration in the presence of nonane vapor, which they partially attributed to incomplete thermalization of the water clusters due to nonane condensation. Similar to the observation by Wagner and Strey,[13] they also observed the inhibition of water condensation onto nucleated particles, likely caused by increased droplet temperature due to nonane condensation and the formation of a hydrophobic surface layer. Chen and co-workers[18–20] calculated the nucleation free energy surface of the aforementioned mixtures via a specifically developed type of biased Monte Carlo simulation. They confirmed the two-pathway mechanism for the water–nonane systems in their simulation, noting that water and nonane exhibit a microscopic immiscibility. These works show that nonane does not enhance water nucleation in the investigated temperature range (196–230 K), and the condensation of water on nucleated particles could be hindered by nonane.

Missing in prior studies are nucleation experiments at lower temperatures and the direct measurement of the composition of the nucleating cluster at the molecular level. The former is valuable as the interspecies interaction—although weak between water and nonane—could potentially play a more important role in nucleation as its relative magnitude compared with the thermal energy increases. Consequently, experimental results conducted at higher temperatures cannot be simply extrapolated to low temperature regimes. The measurement of the composition of nucleating clusters helps clarify the nucleation pathways and provides direct molecular evidence on interspecies interactions by identifying heteromolecular clusters. In this work, we set out to investigate the binary water–nonane system on the molecular level with a special setup based on mass spectrometry,[21] which was designed to measure the composition of weakly bound molecular clusters during nucleation events. The experiments are conducted in the temperature range of 50–110 K, which is significantly lower than the temperature of previous experimental investigations. Binary and unary nucleation measurements are compared in order to elucidate the role of heteromolecular water–nonane clusters during nucleation.

II. EXPERIMENTAL METHODS

The experimental setup has been described in detail in our previous publications.[5,12,21] A brief summary is given here. We use a pulsed supersonic Laval expansion to produce a supersaturated vapor in the post-nozzle flow, which is uniform in temperature and pressure. The vapor is diluted in a carrier gas, which is argon (PanGas 5.0) or nitrogen (PanGas 5.0), and whose expansion determines the temperature of the post-nozzle flow. A small amount of methane (Air Liquide 5.5) is also added as an internal standard to determine absolute cluster concentrations. Water vapor is introduced via a liquid flow meter, and nonane vapor is added via a temperature regulated bubbler, where nonane vapor is picked up by the flowing carrier gas. The vapor concentrations and experimental parameters for the different measurements are listed in Table I. We verify experimentally that nucleation and cluster growth of water and/or nonane take place in the uniform post-nozzle flow. The core of the flow, which contains the molecular clusters formed during nucleation, is sampled with a skimmer and transferred into high vacuum for cluster detection via soft single photon ionization (with an energy of 13.8 eV) coupled with time-of-flight mass spectrometry. We integrate the ion signal and calculate the absolute number concentrations of individual clusters with the methane signal as a reference using the known flow composition and the ionization cross sections of the different species at 13.8 eV. For water, nonane, and methane, the used ionization cross sections are σ_{H_2O} = 42 Mb (based on Haddad and Samson[22]), $\sigma_{C_9H_{20}}$ = 200 Mb (estimated by extrapolating the data from Kameta *et al.*[23]), and σ_{CH_4} = 16.6 Mb (based on Kameta *et al.*[23]), respectively. The ionization cross section for a cluster composed of n molecules of a certain species is assumed to be n times the cross section of the respective monomer (based on theoretical considerations). Upon ionization, a fast proton transfer takes place for water clusters, and an OH-radical is ejected from the cluster.[24,25] The detected water cluster mass peaks are thus shifted down by ~17 m/z, which was taken into account in the assignment of the cluster sizes. The vacuum ultraviolet (VUV) ionization is expected to produce singly charged ions, and no sign of multiple charges was found in the spectra.

We track the evolution of the cluster mass spectra as a function of nucleation time, which was varied by adjusting the distance

TABLE I. Experimental parameters at three different flow temperatures, the nucleation rate J, and the net dimer formation rate constant $k_{1,1}$. The nozzles are labeled by their nominal Mach number, consistent with our earlier publications. The actual Mach number depends among others on the type of carrier gas and is also given. $\ln(S)$ is the natural logarithm of the supersaturation, calculated with the Wagner equation.[27] C_1 denotes the monomer number concentration. The superscripts of J and $k_{1,1}$ indicate the substance, and the subscript indicates whether the nucleation rate was evaluated during nucleation of the unary system or the binary water–nonane system.

Flow temperature (K)	51 ± 1	88 ± 1	108 ± 2
Nozzle/Mach number	M4.0/3.8	M4.0/3.4	M3.0/2.9
Carrier gas	Ar	N_2	N_2
Flow pressure (Pa)	40	42	75
$\ln(S^{H_2O})$	94	40	28
$\ln(S^{C_9H_{20}})$	117	49	32
$C_1^{CH_4}$ (10^{14} cm^{-3})	2.4	1.5	2.1
$C_1^{H_2O}$ (10^{14} cm^{-3})	1.0	2.5	5.1
$C_1^{C_9H_{20}}$ (10^{12} cm^{-3})	2.9	7.6	17
$J_{unary}^{H_2O}$ (10^{15} cm^{-3} s^{-1})	4.1	4.2	7.2
$J_{binary}^{H_2O}$ (10^{15} cm^{-3} s^{-1})	3.3	5.2	6.6
$J_{unary}^{C_9H_{20}}$ (10^{15} cm^{-3} s^{-1})	0.53	0.97	2.0
$J_{binary}^{C_9H_{20}}$ (10^{15} cm^{-3} s^{-1})	0.61	0.86	2.4
$k_{1,1,unary}^{H_2O}$ (10^{-14} cm^3 s^{-1})	41	6.5	2.8
$k_{1,1,binary}^{H_2O}$ (10^{-14} cm^3 s^{-1})	32	8.1	2.5
$k_{1,1,unary}^{C_9H_{20}}$ (10^{-11} cm^3 s^{-1})	6.5	1.7	0.72
$k_{1,1,binary}^{C_9H_{20}}$ (10^{-11} cm^3 s^{-1})	7.4	1.5	0.90

between the nozzle exit and the skimmer. The nucleation time t is determined by dividing this distance by the speed of the post-nozzle flow, with $t = 0$ set to the onset of nucleation, i.e., the point in time when the first cluster signal is detected. The nucleation rate is experimentally determined from the slope of a linear fit of the summed cluster number concentrations with respect to time,

$$J = \frac{\mathrm{d}\sum_{n=n_0}^{\infty} C_n}{\mathrm{d}t}, \tag{1}$$

where C_n is the concentration of cluster n. The dimer formation is considered as the nucleation step for both water and nonane. Therefore, n_0 is set to 2 in the calculation of the nonane nucleation rate. For water, however, a complicating factor arises as the nonane monomer fragments upon ionization and the fragment signals overlap with cluster signals of $(H_2O)_{n<9}$. The overlap makes a quantitative evaluation of $(H_2O)_{n<9}$ cluster concentrations unfeasible. For consistency, the water nucleation rate is thus reported for $n_0 = 9$ (at 51 K) or 10 (at 88 and 108 K) in both unary and binary nucleation experiments. From unary water nucleation experiments, in which water cluster measurements are not affected by nonane, we found that the nucleation rate for $n_0 = 9$ is ~20% lower than the nucleation rate for $n_0 = 3$ when all detectable clusters were included in the calculation. Equation (1) neglects the influence of cluster coagulation. As the cluster concentration increases, cluster coagulation might play a role and thus affect the accuracy of Eq. (1). At the highest cluster concentration observed in our experiments (i.e., 110 K with t = 91 μs), we estimated that the coagulation rate is about 20% of the nucleation rate. To exclude the influence of coagulation on J, we selectively fit the cluster number concentrations measured at shorter nucleation times ($t < 60$ μs) when the cluster concentrations are comparatively low and the effect of coagulation is negligible.

In addition to the nucleation rate, two other quantities are calculated and discussed: one is the net dimer formation rate $k_{1,1}$ and the other is the cluster growth rate enhancement factor η. The nucleation rate is related to the net dimer formation rate constant $k_{1,1}$[26] by

$$J = k_{1,1} C_1^2. \tag{2}$$

Compared with J, $k_{1,1}$ is a better indicator for the influence of temperature on the nucleation process since it normalizes the nucleation rate by the vapor concentrations squared, which is proportional to the monomer–monomer collision frequency at a given temperature. The cluster growth rate enhancement factor η is cluster size dependent and is given by

$$\eta_n = \frac{k_{1,n}}{k_{1,n}^{\mathrm{HS}}}, \tag{3}$$

where $k_{1,n}^{\mathrm{HS}}$ is the hard sphere (HS) collision rate constant between the monomer and cluster n, and $k_{1,n}$ is the experimental cluster growth rate constant calculated with[10]

$$k_{1,n} = \frac{\sum_{i=n+1}^{\infty} C_i(t = t_{\max}) - C_i(t = 0)}{\int_0^{t_{\max}} C_1 C_n \mathrm{d}t}. \tag{4}$$

Our previous study[12] has shown that η_n can be increased by introducing a second, growth enhancing species into the system. Here, we use η_n to indicate the extent to which the introduction of nonane can enhance water cluster growth and vice versa.

Nucleation measurements were conducted at three different temperatures, i.e., 51, 88, and 108 K (determined via Pitot tube measurements, see Table I for more experimental details). At each temperature, cluster mass spectra during unary water nucleation, unary nonane nucleation, and binary water–nonane nucleation were recorded. At a given temperature, the vapor concentrations of water and nonane in the binary experiments are the same as the vapor concentration used in the respective unary nucleation experiments.

III. RESULTS AND DISCUSSION

Figure 1 shows example mass spectra measured at 88 K at four different nucleation times, i.e., four different distances between the nozzle exit and the skimmer. The mass spectra of water and nonane clusters from unary nucleation experiments are superimposed ("superimposed") to facilitate comparison with the mass spectra from the binary nucleation ("binary"). The blue and red vertical lines show the position of homomolecular water and nonane clusters, respectively. Any mass peaks not on these lines would correspond to heteromolecular clusters, but none are detected. Figure 1 shows that the "superimposed" spectra match well with the "binary" spectra, with deviations of the two traces within our measurement uncertainty. Such close agreement was observed for experiments conducted at 88 and 108 K. At 51 K, the deviations between "superimposed" and "binary" spectra are slightly more pronounced than shown in Fig. 1; we will come back to that in the quantitative discussion below.

We next compare the nucleation rates to discuss quantitatively whether water and nonane nucleation can be regarded as being independent from each other. Figure 2 (left axis) shows the nucleation rate at different temperatures for both unary and binary nucleation. For the binary nucleation, the nucleation rate of water and nonane can be evaluated separately since heteromolecular clusters are not observed (see Fig. 1). As nucleation transitions from unary to binary, the water nucleation rate changes by −20%, +24%, and −8.3% at 51, 88, and 108 K, respectively (see Table I for the absolute values of the nucleation rates). The corresponding change of nonane nucleation is +15%, −11%, and +20%. This change of the nucleation rates does not appear systematic, rather pointing to experimental scatter as the source of variation than to any apparent nucleation enhancing or suppressing effects. The extent of the variation is also within our measurement uncertainty, which could be caused by fluctuations of the flow temperature, the vapor concentrations, and the ionization laser intensity. The minor differences between the nucleation rates of the unary and binary systems indicate that water and nonane nucleation can be regarded as mutually independent. This independence is in line with the study by Wagner and Strey[13] conducted at 230 K with higher vapor concentrations but is in stark contrast to our previous investigations of the CO_2-containing systems where the addition of CO_2 drastically increases the nucleation rates of several species (toluene, water, etc.) even though CO_2 does not nucleate by itself.[12]

While the nucleation rates of water and nonane change by no more than a factor of four from 51 to 108 K, this does not reflect the influence of temperature on the nucleation process because we use higher vapor concentration at higher temperatures to keep the

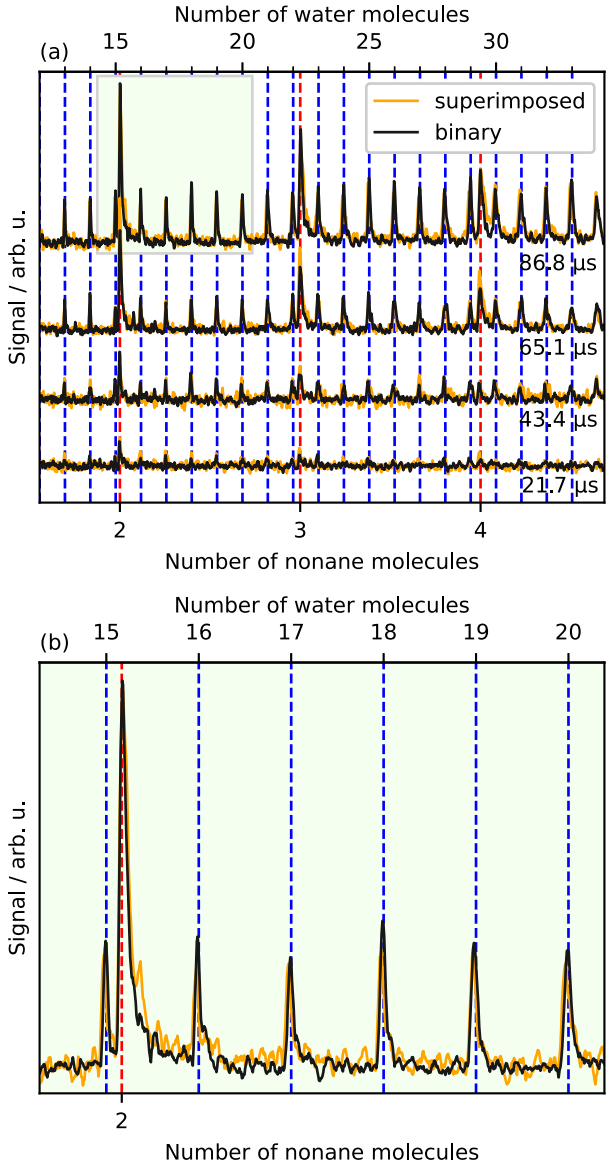

FIG. 1. (a) The mass spectra measured in the unary and binary nucleation experiments at $T = 88$ K. The spectra from the unary experiments are superimposed for comparison with the binary spectra. (b) A zoomed-in version of the green area in (a) for clearer visualization. The blue and red dashed lines show the position of the water and nonane clusters, respectively.

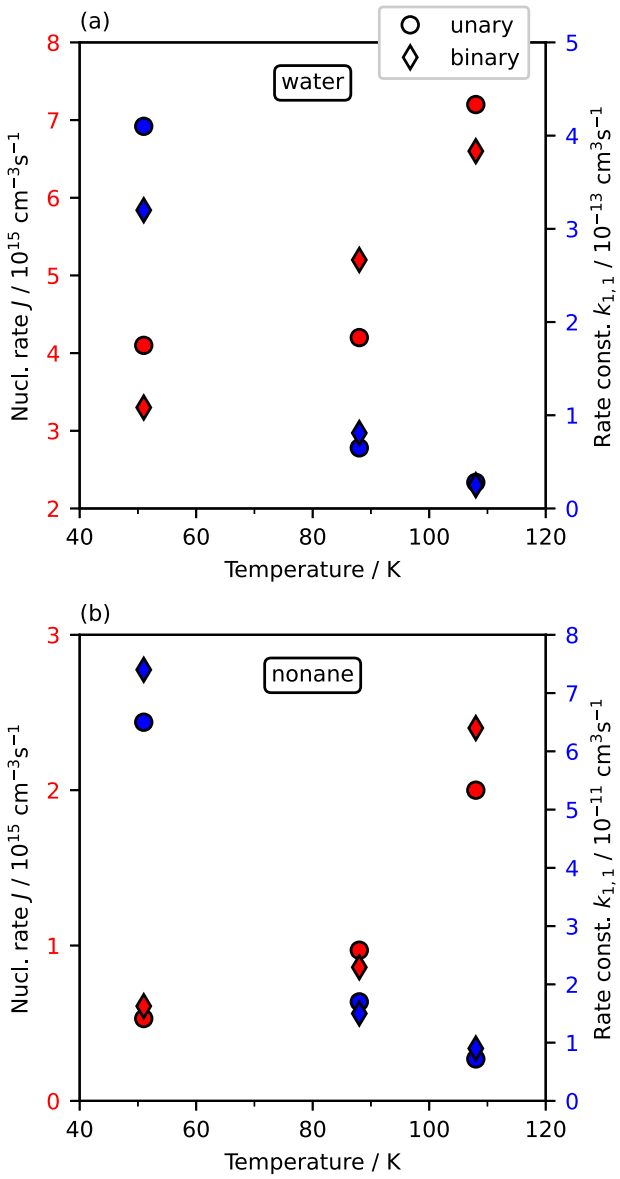

FIG. 2. The nucleation rates J (left axis, red symbols) and the net dimer formation rate constants $k_{1,1}$ (right axis, blue symbols) of water (a) and nonane (b) for both unary and binary nucleation.

cluster signal above the instrument's detection limit. Figure 2 (right axis) shows the net dimer formation rate constant $k_{1,1}$, which is a better indicator of the temperature effect (see Sec. II). Figure 2 shows that for both water [Fig. 2(a)] and nonane [Fig. 2(b)], $k_{1,1}$ decreases by approximately an order of magnitude with the increasing flow temperature over the temperature range of our experiments. Although quite pronounced, the decrease of $k_{1,1}$ observed here is still considerably weaker than the one observed for more weakly bound molecules, such as CO_2, where $k_{1,1}$ drops by several orders of magnitude over an even smaller increase of temperature (e.g., $k_{1,1}$ for CO_2 decreases by 4 orders of magnitude from 31 to 63 K) due to the emergence of a nucleation barrier.[26] The intermolecular interaction between like molecules is stronger for water and nonane molecules than for CO_2, which might prevent the emergence of an apparent nucleation barrier in the investigated temperature range. The decrease of $k_{1,1}$ for water/nonane at higher temperatures might arise from an increase in the evaporation rates of the smallest clusters, e.g., the spontaneous dissociation of a formed dimer.

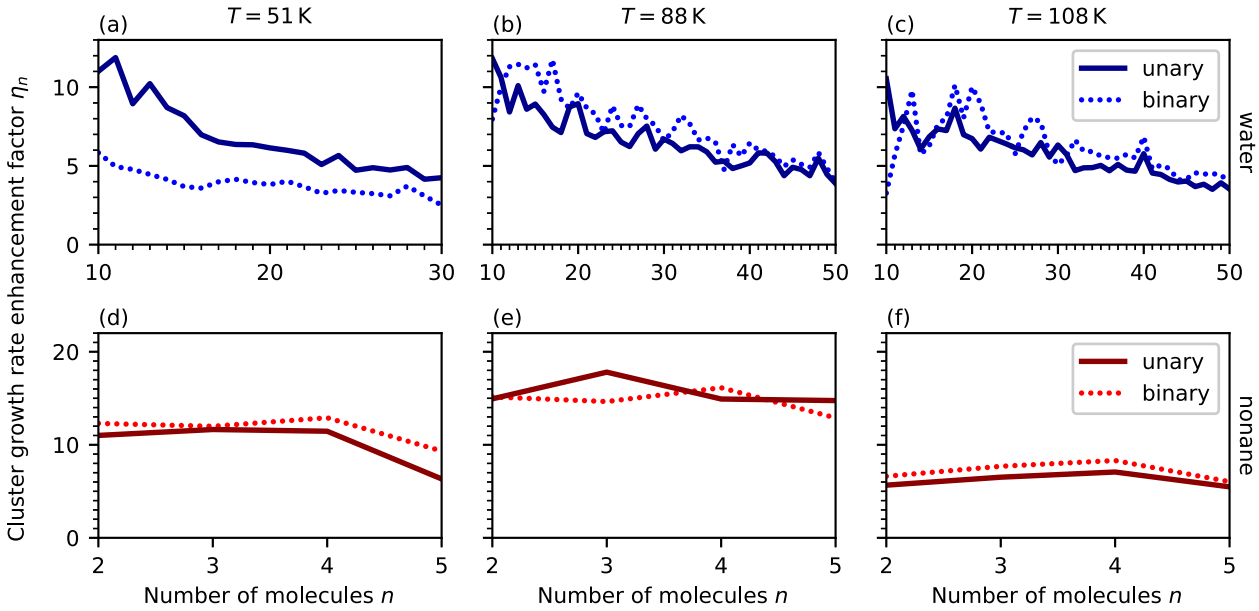

FIG. 3. Size resolved cluster growth enhancement factor η_n for water and nonane at three different temperatures. (a)–(c) Comparison of η_n for water clusters during unary and binary nucleation at temperatures of 51, 88, and 108 K, respectively. (d)–(f) are the same as (a)–(c) but for nonane clusters.

Another possible explanation might be insufficient collisional cooling of the monomer–monomer/cluster collision complex, which results in sticking efficiencies below unity, decreasing further with increasing temperature.[28,29]

Finally, we evaluated the growth rate enhancement factor η_n calculated with Eqs. (3) and (4), which is shown in Fig. 3. Except in panel (a), the differences of η_n between the unary and binary experiments are small and non-systematic, which suggests that neither species plays a significant role during cluster growth of the other species. We note that the values of η_n for unary water nucleation are in the range of 5–12 for $10 \le n \le 30$, which is larger than our previously reported value of 4–5.[10] The larger η might be caused by an increase in the cluster detection efficiency as we shortened the length of the differential pumping chamber between the skimmer and the time-of-flight chamber after our previous publication.

Distinct from other panels, Fig. 3(a) shows a systematic decrease of η_n for water cluster growth by up to a factor of two for small clusters after nonane is introduced into the system at 51 K. Such a negative influence can likely be attributed to nonane molecules adsorbing to the water cluster surface and hindering further water condensation by making parts of the cluster surface inaccessible to condensing water molecules. This observation is similar to what was observed by Wagner and Strey[13] as well as by Pathak *et al.*[17] at higher temperatures and vapor concentrations, but with two distinctions. First, the inhibiting effect of nonane on water condensation was observed for particles above 3 nm in previous studies,[13,17] but here, the inhibiting effect is observed for water clusters containing much fewer molecules, i.e., down to 10. Second, in previous reports, the condensed phase contains a considerable fraction of nonane, but here, in our experiments, the nonane molecules only temporarily adsorb to the water clusters since we do not observe heteromolecular clusters in the mass spectra. The adsorption of nonane to water clusters must be transient with its lifetime shorter than the time scale of our experiment (~500 μs).

IV. CONCLUSION

We have conducted molecular-level nucleation experiments of water, nonane, and their mixtures in the temperature range of 50–110 K. Overall, our measurements suggest that the nucleation of these two substances proceeds along independent pathways, which is supported by the near identical nucleation rates during unary and binary nucleation. This independence was also observed in a prior study conducted at a temperature of 230 K. Together, these studies suggest that at atmospherically relevant conditions, water and nonane (or alkanes with similar chain length) are unlikely to cooperate to enhance nucleation. For cluster growth, we did not observe evidence of interspecies interactions influencing cluster growth at 88 K or above. At 51 K, nonane cluster growth is still not affected by water, but the water cluster growth rate appears to be slowed by a factor of approximately two in the presence of nonane. This might be explained by transient adsorption of nonane molecules temporarily blocking part of the surface of the water clusters. The water–nonane vapor mixture is a model system in which the interspecies intermolecular interactions are weaker than intraspecies interactions. This work shows that such weak interspecies interactions barely affect the phase transition of both species at temperatures at 88 and 108 K at the investigated vapor concentration. However, its influence on cluster growth begins to emerge at 51 K. Further investigations at

even lower temperatures might thus reveal more complex behaviors of the water–nonane nucleation system.

ACKNOWLEDGMENTS

This project was supported by the Swiss National Science Foundation (SNSF Project No. 200020_200306), ETH Zürich, and the Natural Science Foundation of Shanghai (Grant No. 21ZR1430100). We express our gratitude to E. Chasovskikh and B. Yoder for help with the maintenance of the experimental setup and to D. Stapfer and M. Steger from our workshops for technical support.

AUTHOR DECLARATIONS

Conflict of Interest

The authors have no conflicts to disclose.

Author Contributions

S.F. and J.K. contributed equally to this work.

Stefan Feusi: Data curation (equal); Formal analysis (equal); Investigation (equal); Software (equal); Validation (equal); Visualization (equal); Writing – review & editing (equal). **Jan Krohn**: Data curation (equal); Formal analysis (equal); Investigation (equal); Software (equal); Validation (equal); Visualization (equal); Writing – original draft (equal). **Chenxi Li**: Conceptualization (equal); Funding acquisition (equal); Investigation (equal); Supervision (equal); Validation (equal); Writing – review & editing (equal). **Ruth Signorell**: Conceptualization (equal); Data curation (equal); Funding acquisition (equal); Methodology (equal); Project administration (equal); Resources (equal); Supervision (equal); Validation (equal); Writing – review & editing (equal).

DATA AVAILABILITY

The data that support the findings of this study are openly available in the ETH Research Collection at https://doi.org/10.3929/ethz-b-000584229.

REFERENCES

[1] S. M. Burrows, C. S. McCluskey, G. Cornwell, I. Steinke, K. Zhang, B. Zhao, M. Zawadowicz, A. Raman, G. Kulkarni, S. China, A. Zelenyuk, and P. J. DeMott, Rev. Geophys. **60**, e2021RG000745, https://doi.org/10.1029/2021rg000745 (2022).
[2] J. Haywood and O. Boucher, Rev. Geophys. **38**, 513, (2000).
[3] M. Z. Jacobson, J. Geophys. Res.: Atmos. **106**, 1551, (2001).
[4] C. J. Hennigan, M. H. Bergin, J. E. Dibb, and R. J. Weber, Geophys. Res. Lett. **35**, L18801, https://doi.org/10.1029/2008gl035046 (2008).
[5] M. Lippe, S. Chakrabarty, J. J. Ferreiro, K. K. Tanaka, and R. Signorell, J. Chem. Phys. **149**, 244303 (2018).
[6] R. H. Heist and H. Reiss, J. Chem. Phys. **59**, 665 (1973).
[7] J. Wölk and R. Strey, J. Phys. Chem. B **105**, 11683 (2001).
[8] B. E. Wyslouzil and J. Wölk, J. Chem. Phys. **145**, 211702 (2016).
[9] J. Wölk, R. Strey, C. H. Heath, and B. E. Wyslouzil, J. Chem. Phys. **117**, 4954 (2002).
[10] C. Li, M. Lippe, J. Krohn, and R. Signorell, J. Chem. Phys. **151**, 094305 (2019).
[11] J. H. Zollner, W. A. Glasoe, B. Panta, K. K. Carlson, P. H. McMurry, and D. R. Hanson, Atmos. Chem. Phys. **12**, 4399 (2012).
[12] C. Li, J. Krohn, M. Lippe, and R. Signorell, Sci. Adv. **7**, eabd9954 (2021).
[13] P. E. Wagner and R. Strey, J. Phys. Chem. B **105**, 11656 (2001).
[14] R. Strey, Y. Viisanen, and P. E. Wagner, J. Chem. Phys. **103**, 4333 (1995).
[15] Y. Viisanen, R. Strey, A. Laaksonen, and M. Kulmala, J. Chem. Phys. **100**, 6062 (1994).
[16] Y. Viisanen, P. E. Wagner, and R. Strey, J. Chem. Phys. **108**, 4257 (1998).
[17] H. Pathak, J. Wölk, R. Strey, and B. E. Wyslouzil, J. Chem. Phys. **140**, 034304 (2014).
[18] R. B. Nellas, S. J. Keasler, and B. Chen, J. Phys. Chem. A **112**, 2930 (2008).
[19] R. B. Nellas, M. E. McKenzie, and B. Chen, J. Phys. Chem. B **110**, 18619 (2006).
[20] B. Chen, J. I. Siepmann, and M. L. Klein, J. Am. Chem. Soc. **125**, 3113 (2003).
[21] B. Schläppi, J. H. Litman, J. J. Ferreiro, D. Stapfer, and R. Signorell, Phys. Chem. Chem. Phys. **17**, 25761 (2015).
[22] G. N. Haddad and J. A. R. Samson, J. Chem. Phys. **84**, 6623 (1986).
[23] K. Kameta, N. Kouchi, M. Ukai, and Y. Hatano, J. Electron Spectrosc. Relat. Phenom. **123**, 225 (2002).
[24] L. Belau, K. R. Wilson, S. R. Leone, and M. Ahmed, J. Phys. Chem. A **111**, 10075 (2007).
[25] H. Tachikawa, J. Phys. Chem. A **108**, 7853 (2004).
[26] J. Krohn, M. Lippe, C. Li, and R. Signorell, Phys. Chem. Chem. Phys. **22**, 15986 (2020).
[27] Verein Deutscher Ingenieure, VDI-Gesellschaft Verfahrenstechnik, and Chemieingenieurwesen, *VDI-Wärmeatlas* (Springer, 2006).
[28] J. Bourgalais, V. Roussel, M. Capron, A. Benidar, A. W. Jasper, S. J. Klippenstein, L. Biennier, and S. D. Le Picard, Phys. Rev. Lett. **116**, 113401 (2016).
[29] J. Feder, K. C. Russell, J. Lothe, and G. M. Pound, Adv. Phys. **15**, 111 (1966).